2023 IEEE Conference on Control Technology and Applications (CCTA)
August 16-18, 2023. Bridgetown, Barbados

Stochastic Planning of a Mostly-Renewable Power Grid

Sunny Chen, Johanna L. Mathieu, and Peter Seiler

2023 IEEE Conference on Control Technology and Applications (CCTA) | 979-8-3503-3544-6/23/$31.00 ©2023 IEEE | DOI: 10.1109/CCTA54093.2023.10253007

Abstract— **Power grid resource adequacy can be difficult to ensure with high penetrations of intermittent renewable energy. We explore enhancing resource adequacy by overbuilding renewables while modeling statistical correlations in renewable power at different sites. Overbuilding allows production during times of low power, and exploiting statistical correlations can reduce power variability and, subsequently, reduce needed renewable capacity. In this work, we present a stochastic optimization problem to size renewables and expand transmission while minimizing the expected dispatch cost. Our method uses statistical profiles of renewable production and embeds network constraints using the DC power flow equations. We assess our method's effects on feasibility, load shedding, locational marginal prices, and generator curtailment. On the IEEE 9-bus system, we found that anti-correlation between generators reduced generation capacity needs with sufficient transmission. On the IEEE 30-bus system, we found that the optimal solution required significant overbuilding and curtailment of renewables regardless of the marginal cost of schedulable generation.**

I. Introduction

Countries have begun to decarbonize their electricity sectors to counter climate change [1]. Many are moving to intermittent renewable power sources, e.g., wind and solar. To integrate intermittent power into the grid, system operators must cope with both forecasted changes in renewable power, termed variability, and unforecasted deviations, termed uncertainty. Traditionally, system operators handle variability by scheduling fast-ramping flexible resources [2], such as gas power plants, hydropower plants, or energy storage. As gas is phased out, hydropower growth is limited, and renewable penetrations are increased, the need for flexibility will grow, leading many to posit that energy storage is the only solution. Here, we consider an alternative where we overbuild renewable capacity and dispatch renewables themselves for flexibility. Overbuilding renewables may be less expensive and/or greener than energy storage-based solutions, especially those using chemical batteries.

One method to reduce the variability of renewables is to build complementary resources. Complementarity refers to spatial or temporal correlations in energy production at different renewable sites [3]. Sites with weakly- or anti-correlated energy production will exhibit reduced aggregate variability compared to highly correlated sites. For example, [4] uses complementarity in designing reliable renewable hybrid power stations.

In this paper, we investigate how statistical correlation of renewable energy production at various sites affects generation planning, transmission planning, and dispatch in mostly-renewable power grids, defined here as grids dominated by variable renewables, with only a small amount of traditional (schedulable) generation. To do this, we formulate a two-stage stochastic program that co-optimizes renewable generation and transmission expansion, and then solves for associated optimal dispatch schedules, including renewable generation curtailment. The first stage minimizes the construction cost, and the second stage minimizes expected load shedding and generation costs while accounting for line limits. Our aim is two-fold: 1) to provide a method to co-optimize renewable capacity and transmission planning under complementarity; and 2) to analyze the optimal dispatch of complementary renewables.

One approach to capacity planning is to manipulate time series of renewable power potentials. Ref. [5] uses European wind, solar, and demand time series to find a wind-solar mix that meets variable demand at minimum capacity. Ref. [6] uses time series to form probability distributions of renewable power forecast error to determine reserve requirements. These approaches model net power imbalance but do not consider network constraints.

Other works analyze the use of energy storage to mitigate renewable variability. Ref. [7] sites and sizes energy storage by solving a series of unit commitment problems to maximize the usage of wind and minimize the cost of other generation. Ref. [8] presents a probabilistic method that calculates the expected energy not served for a hybrid wind-and-storage generator. These papers solve a similar problem of mitigating renewable variability, but they do not consider how renewables themselves may be sized for flexibility.

Some papers have proposed power and reserve dispatch strategies that ensure reliability and security under renewable forecast errors. Ref. [9] presents a chance-constrained optimal power flow (OPF) that accounts for line flow limit violations from generators compensating forecast error. Ref. [10] formulates a chance-constrained OPF to schedule reserves under $N-1$ security constraints and wind power forecast error. Both approaches embed network constraints into their optimization problems via the DC power flow equations, but solve a scheduling and real-time control problem, not a planning problem, and do not include renewable curtailment.

Other research explores the use of optimization in planning decarbonization pathways with renewables and energy storage. Refs. [11], [12] formulate multi-stage stochastic optimization problems to co-optimize generation, storage, and transmission investment while accounting for power variability using scenarios. These works account for complementarity, changing energy usage patterns, and transmission

This work was partially supported by US NSF Award 1845093.

The authors are with the Department of Electrical Engineering and Computer Science, University of Michigan, Ann Arbor, MI 48109, USA {chensunn, pseiler, jlmath}@umich.edu

constraints in real-time operation but do not analyze the effects of complementarity on dispatch.

The contribution of this paper is an exploration of how renewable complementarity affects grid planning and dispatch in a mostly-renewable grid in which renewables, not storage, provide flexibility. We develop a two-stage stochastic optimization problem minimizing the cost of construction and operation, and we use sampled scenarios to capture variability. To model line flow constraints and power balance, we use the DC power flow equations. To capture randomness in renewable generation across multiple sites and time periods, we model renewable generation capacities as random variables. We also model correlation in energy production between sites. Lastly, we test our planning problem solutions by dispatching the system with a DC OPF, and assess performance.

The remainder of the paper is organized as follows. Section II outlines our problem setup and assumptions. Section III formulates our stochastic planning algorithm. Section IV contains case studies on the IEEE 9- and 30-bus systems. We conclude the paper and comment on future work in Section V.

II. Problem Description

We consider the problem of constructing renewable capacity to minimize construction and operational costs under uncertain power generation and demand. Our network has N_{bus} buses, N_{var} renewable generation sites, N_{sch} schedulable generators, N_{line} lines in set $\mathcal{L}$, and N_{load} loads. Time-varying energy and load statistics are indexed by time periods $t = 1, \ldots, N_{\text{times}}$. Multiple generation sites or loads can be attached to a bus.

We now discuss how we model generation and transmission capacity. To model renewable capacity, we let $P^{\max}_{\text{var},i}$ be the max renewable capacity that can be built at site i and $0 \leq x_{1,i} \leq 1$ be the built proportion of max capacity at site i. At $x_{1,i} = 0$, no capacity is built, while at $x_{1,i} = 1$, we can extract max possible power. To model transmission expansion on the line connecting buses i and j, we define f_{ij} as the initial max transmission capacity on line i-j, f^{add}_{ij} as the max additional transmission capacity on line i-j, and $0 \leq x_{2,ij} \leq 1$ as the built proportion of additional transmission capacity on line i-j. At $x_{2,ij} = 0$, no additional transmission capacity is built, while at $x_{2,ij} = 1$, the max possible additional transmission capacity is built. We only model transmission expansion on existing links and assume that new links cannot be built.

We conceptualize a two-stage problem where the first stage decides renewable generation and transmission capacity, and the second stage decides hourly dispatch of renewable generation (i.e., curtailment), schedulable generation, and load shedding. We stack $x_{1,i}\,\forall i$ and $x_{2,ij}\,\forall i$-j into the decision variables x_1 and x_2, respectively. In the second stage, we dispatch the system according to realized values of load and max renewable generation. We only model hourly variability, not forecast error or variability in other timescales. We formulate the problem of constructing renewable capacity as

$$\min_{x_1,x_2} \; c_1^\top x_1 + c_2^\top x_2 + \mathcal{Q}(x_1, x_2) \tag{1}$$

$$\text{s.t. } 0 \leq x_1 \leq 1, \tag{2}$$

$$0 \leq x_2 \leq 1, \tag{3}$$

where $\mathcal{Q}(x_1, x_2)$ is the optimal operational cost given x_1 and x_2. In practice, it depends on random variables. Here, c_1 is the renewable capacity construction cost, and c_2 is the transmission capacity construction cost. In Section III, we formulate a two-stage stochastic program to solve this optimization problem.

To model randomness in max renewable power, we let $P_t = [P_{1,t}, \ldots, P_{N_{\text{var}},t}]^\top \in \mathbb{R}^{N_{\text{var}}}$ be a random vector where the ith element represents the max possible power generation at site i at timestep t. Similarly, we let $D_t = [D_{1,t}, \ldots, D_{N_{\text{load}},t}]^\top \in \mathbb{R}^{N_{\text{load}}}$ be a random vector of the power demand at each load at timestep t. We use the convention that elements of P_t and D_t are non-negative. To model correlations, we assume

$$(P_1, \ldots, P_{N_{\text{times}}}, D_1, \ldots, D_{N_{\text{times}}}) \sim \mathcal{P}, \tag{4}$$

i.e., that all renewable generation capacities and loads are jointly distributed according to some distribution $\mathcal{P}$. We let $x_1 \odot P_t$ model the max power generation, where $\odot$ is the Hadamard (element-wise) product. Let Ω be the scenario set, i.e., $P_t(\omega), D_t(\omega)$ are realizations of events $\omega \in \Omega$.

If the power demand is nonzero but the available renewable power is zero, then no feasible dispatch exists for any amount of constructed renewables. To avoid this, we include a small amount of schedulable generation (that can be arbitrarily dispatched within constant generator limits) and load shedding. The schedulable generator could be a traditional fossil-fuel plant or a renewable resource such as hydropower. We let $P_{\text{sch},t}$ be the power dispatch for schedulable generation at timestep t. Similarly, we define load shedding as the ability to reduce demand to ensure power balance. We denote $P_{\text{load},t}$ as the power dispatch for a load at timestep t. To account for the costs of dispatching schedulable generation and load shedding in the planning algorithm, we must minimize their expected costs together with the cost of renewables and transmission expansion.

To model power flow, we must map the power from variable generators, schedulable generators, and loads to bus injections. We do this by defining matrices M_{var}, M_{sch}, and M_{load}, where their (i, j) elements are

$$(M_{\text{var}})_{ij} = \begin{cases} 1, & \text{for variable generator } j \text{ on bus } i \\ 0, & \text{elsewhere,} \end{cases} \tag{5}$$

$$(M_{\text{sch}})_{ij} = \begin{cases} 1, & \text{for sched. generator } j \text{ on bus } i \\ 0, & \text{elsewhere,} \end{cases} \tag{6}$$

$$(M_{\text{load}})_{ij} = \begin{cases} 1, & \text{for load } j \text{ on bus } i \\ 0, & \text{elsewhere.} \end{cases} \tag{7}$$

Then, the bus power injection vector P_{bus} can be written as $P_{\text{bus}} = M_{\text{var}} P_{\text{var}} + M_{\text{sch}} P_{\text{sch}} - M_{\text{load}} P_{\text{load}}$. We define the bus power injection as positive when power is generated.

To account for line constraints, we use the DC power flow equations, which linearly approximate full AC power flow but do not capture reactive power, active power losses, or voltage magnitudes. Although the equations are approximate, we use them because they are linear and can thus be used in convex optimization problems. The DC power flow equations are

$$B\theta = P_{\text{bus}}, \tag{8}$$

$$|(B)_{ij}(\theta_i - \theta_j)| \leq f_{ij} + f_{ij}^{\text{add}} x_{2,ij}, \forall (i,j) \in \mathcal{L}, \tag{9}$$

where (8) relates P_{bus} to voltage angles θ via the susceptance matrix B and ensures power balance, and (9) imposes line power flow limits, where $f_{ij} + f_{ij}^{\text{add}} x_{2,ij}$ relates available transmission capacity to the first-stage decision, $x_{2,ij}$. Constraint (9) can be split into two linear constraints.

Lastly, we make the following additional assumptions. First, we assume no further schedulable generation capacity can be built. Second, we do not use inter-period constraints, such as ramping or unit commitment (on/off) constraints.

III. Two-Stage Stochastic Program

Here, we describe the two-stage stochastic program. Our first-stage decision sets x_1 and x_2, the renewable generation capacity and added transmission. In the second stage, we observe the event $\omega \in \Omega$ realized in random variables $(D_1(\omega), D_2(\omega), \ldots, D_{N_{\text{times}}}(\omega))$ and $(P_1(\omega), P_2(\omega), \ldots, P_{N_{\text{times}}}(\omega))$, i.e., the load and max possible renewable generation per timestep. Then, we take recourse as a dispatch $(P_{\text{sch},t}(\omega), P_{\text{load},t}(\omega), P_{\text{var},t}(\omega), \theta_t(\omega))$ that satisfies the DC power flow equations and does not exceed $x_1 \odot P_t(\omega)$, the max possible renewable generation for ω and t. Our notation indicates that the dispatch depends on ω. Recall the first-stage deterministic program (1)–(3). Letting $\mathbf{y}_2(\omega) = (P_{\text{sch}}(\omega), P_{\text{load}}(\omega), P_{\text{var}}(\omega), \theta(\omega))$ be the second-stage decision variables, the optimal second-stage cost $\mathcal{Q}(x_1, x_2)$ is the optimal objective value of

$$\min_{\mathbf{y}_2(\omega)} \mathbb{E}\left\{ \sum_{t=1}^{N_{\text{times}}} (c_3^\top P_{\text{sch},t}(\omega) + c_4^\top [D_t(\omega) - P_{\text{load},t}(\omega)] \right\} \tag{10}$$

$$\text{s.t. } \forall t = 1, \ldots, N_{\text{times}},$$

$$0 \leq P_{\text{var},t}(\omega) \leq x_1 \odot P_t(\omega), \tag{11}$$

$$0 \leq P_{\text{load},t}(\omega) \leq D_t(\omega), \tag{12}$$

$$0 \leq P_{\text{sch},t}(\omega) \leq P_{\text{sch}}^{\max}, \tag{13}$$

$$B\theta_t(\omega) = M_{\text{var}} P_{\text{var},t}(\omega) + M_{\text{sch}} P_{\text{sch},t}(\omega) - M_{\text{load}} P_{\text{load},t}(\omega), \tag{14}$$

$$|(B)_{ij}(\theta_{i,t}(\omega) - \theta_{j,t}(\omega))| \leq f_{ij} + f_{ij}^{\text{add}} x_{2,ij}, \forall (i,j) \in \mathcal{L}. \tag{15}$$

Here, c_3 is the marginal cost of schedulable generation, and c_4 is the cost of load shedding, both of which we assume to be linear costs. Also, $P_{\text{sch}}^{\max}$ is the max power output of schedulable generation. In words, $\mathcal{Q}(x_1, x_2)$ is the expected cost of the DC OPF given a decision x_1 and x_2 under variability in P_t and D_t. Our two-stage problem consists of (1)–(3), corresponding to the first stage, and (10)–(15), corresponding to the second stage.

Finding $\mathcal{Q}(x_1, x_2)$ is generally intractable because Ω is of infinite cardinality. We solve this problem with sample average approximation (SAA). We generate a finite scenario set $\widetilde{\Omega}$ by sampling (4) for each time period, where we use a tilde to mark variables that change in our SAA. We choose the number of samples to well-approximate the actual expected value. We notate scenarios as $\omega^s \in \widetilde{\Omega}$ for $s = 1, \ldots, N_{\text{scen}}$. Each ω^s corresponds to a realization $(D_1^s, D_2^s, \ldots, D_{N_{\text{times}}}^s)$ and $(P_1^s, P_2^s, \ldots, P_{N_{\text{times}}}^s)$. Our second-stage decisions are, for each $\omega^s \in \widetilde{\Omega}$ and time t, an optimal dispatch $(P_{\text{sch},t}^s, P_{\text{load},t}^s, P_{\text{var},t}^s, \theta_t^s)$. We collect these into a vector $\widetilde{\mathbf{y}}_2$. Together with first-stage decisions $\mathbf{y}_1 = (x_1, x_2)$, the two-stage problem (1)–(3), (10)–(15) can be reformulated into the following linear program,

$$\min_{\mathbf{y}_1, \widetilde{\mathbf{y}}_2} \; c_1^\top x_1 + c_2^\top x_2 + \frac{1}{N_{\text{scen}}} \sum_{s=1}^{N_{\text{scen}}} \sum_{t=1}^{N_{\text{times}}} c_3^\top P_{\text{sch},t}^s + c_4^\top (D_t^s - P_{\text{load},t}^s) \tag{16}$$

$$\text{s.t. } 0 \leq x_1 \leq 1, \tag{17}$$

$$0 \leq x_2 \leq 1, \tag{18}$$

$$\forall s = 1, \ldots, N_{\text{scen}}, \; \forall t = 1, \ldots, N_{\text{times}},$$

$$0 \leq P_{\text{var},t}^s \leq x_1 \odot P_t^s, \tag{19}$$

$$0 \leq P_{\text{load},t}^s \leq D_t^s, \tag{20}$$

$$0 \leq P_{\text{sch},t}^s \leq P_{\text{sch}}^{\max}, \tag{21}$$

$$B\theta_t^s = M_{\text{var}} P_{\text{var},t}^s + M_{\text{sch}} P_{\text{sch},t}^s - M_{\text{load}} P_{\text{load},t}^s, \tag{22}$$

$$|(B)_{ij}(\theta_{i,t}^s - \theta_{j,t}^s)| \leq f_{ij} + f_{ij}^{\text{add}} x_{2,ij}, \forall (i,j) \in \mathcal{L}. \tag{23}$$

Eq. (16) defines the objective function. Constraints (17)–(18) limit the buildable renewable generation and transmission capacity. For each scenario, (19)–(21) limit dispatchable power, while (22)–(23) are the DC power flow equations.

IV. Results and Discussion

In this section, we discuss our test setup, results, and solution validation. We solve the optimization problem with Julia, PowerModels.jl [13], JuMP [14], and Gurobi. We set the cost parameters c_1, c_2, c_3, and c_4 and analyze the results. Since we are more interested in the relative costs of various resources, we do not attach currency units to costs.

A. Variability Model

We now describe the probability distributions of renewables and loads. We assume that, for $t = 1, \ldots, N_{\text{times}}$, P_t follows a truncated joint normal distribution with mean $\mu_t \in \mathbb{R}^{N_{\text{var}}}$, covariance $\Sigma_t \in \mathbb{R}^{N_{\text{var}} \times N_{\text{var}}}$, and interval bounds $0 \leq P_t \leq x_1 \odot P_{\text{var}}^{\max}$. We assume that D_t is constant. We also let P_t and D_t be independent across time. We use truncated joint normals, do not model load variation or correlation, and ignore temporal correlations for convenience, but our scenario approach can accept arbitrary distributions, including ones that model these effects differently.

B. Test Metrics

We now describe how we quantify the reliability of our system given optimal x_1 and x_2 obtained from (16)–(23). We conduct our analysis by first obtaining a test scenario set, $\bar{\Omega}$, which is a finite set with N_{testscen} scenarios. Then, for each scenario $\bar{s} = 1, \ldots, N_{\text{testscen}}$, we run the following DC OPF to obtain an optimal dispatch for each time period, $\overline{\mathbf{y}}_t^{\bar{s}} = (P_{\text{sch},t}^{\bar{s}}, P_{\text{load},t}^{\bar{s}}, P_{\text{var},t}^{\bar{s}}, \theta_t^{\bar{s}})$:

$$\min_{\overline{\mathbf{y}}_t^{\bar{s}}} c_3^\top P_{\text{sch},t}^{\bar{s}} + c_4^\top (D_t^{\bar{s}} - P_{\text{load},t}^{\bar{s}}) \tag{24}$$

$$\text{s.t. } 0 \le P_{\text{var},t}^{\bar{s}} \le x_1 \odot P_t^{\bar{s}}, \tag{25}$$

$$0 \le P_{\text{load},t}^{\bar{s}} \le D_t^{\bar{s}}, \tag{26}$$

$$0 \le P_{\text{sch},t}^{\bar{s}} \le P_{\text{sch}}^{\max}, \tag{27}$$

$$B\theta_t^{\bar{s}} = M_{\text{var}} P_{\text{var},t}^{\bar{s}} + M_{\text{sch}} P_{\text{sch},t}^{\bar{s}} - M_{\text{load}} P_{\text{load},t}^{\bar{s}}, \tag{28}$$

$$|(B)_{ij}(\theta_{i,t}^{\bar{s}} - \theta_{j,t}^{\bar{s}})| \le f_{ij} + f_{ij}^{\text{add}} x_{2,ij}, \forall (i,j) \in \mathcal{L}. \tag{29}$$

This problem differs from (10)–(15) since it gives the optimal dispatch at one time period instead of the expected value of optimal dispatch over multiple time periods. Using the DC OPF dispatch, we formulate the following metrics.

1) Feasibility: We define the probability of feasibility as the probability that we can dispatch to serve all loads completely. We determine this from the proportion of scenarios for which DC OPF is feasible with no load shedding.

2) Load shed quantiles: Next, we quantify how much additional capacity is needed to ensure feasibility. First, we calculate the total load shed needed in scenario s and time t, defined as $P_{\text{shed},t}^{\bar{s}} = \mathbf{1}^\top (D_t^{\bar{s}} - P_{\text{load},t}^{\bar{s}})$. Then, we calculate the 0.99 quantile of $P_{\text{shed},t}^{\bar{s}}$ over all scenarios and time periods, which is the total amount of additional power needed for feasibility in 99% of operating periods.

3) LMPs: We define the LMP at each bus as the dual variable of (28), interpreting the dual variable as the additional load shedding induced by increased load served at some bus. LMPs increase with system congestion and lack of energy.

4) Curtailment: We use curtailment to quantify how far a generator is operating from its maximum power. For each scenario s and timestep t, we define schedulable generator i's curtailment as $P_{\text{curt},i,t}^s = (P_{\text{sch},i}^{\max} - P_{\text{sch},i,t})/P_{\text{sch},i}^{\max}$ and renewable generator i's curtailment as

$$P_{\text{curt},i,t}^s = \begin{cases} \frac{x_{1,i,t} P_{i,t}^s - P_{\text{var},i,t}}{x_{1,i,t} P_{i,t}^s}, & P_{i,t}^s \neq 0 \\ 0, & P_{i,t}^s = 0. \end{cases} \tag{30}$$

A generator is producing at maximum when $P_{\text{curt},i,t} = 0$, and it is not producing at all when $P_{\text{curt},i,t} = 1$.

C. IEEE 9-Bus System

We first use a simple test case to isolate the effect of renewable generation correlation on planning and dispatch. We set $N_{\text{times}} = 1$ and use the IEEE 9-bus system from MATPOWER [15], as shown in Fig. 1. All loads have their values from [15]. We let Generator 1 be schedulable and Generators 2 and 3 be variable renewables, so there is one correlation variable. We let the variable generators have 50% capacity factors. The capacity factor is defined as the ratio of max available energy to energy produced at nameplate capacity. We calculate generator i's capacity factor as $(\sum_{t=1}^{N_{\text{times}}} \mathbb{E}[P_{i,t}])/(\sum_{t=1}^{N_{\text{times}}} P_{\text{var},i}^{\max})$. Their power standard deviations are 15% of their max capacity. Table I contains simulation parameters. We calculate the planned generation and transmission capacity while letting the correlation coefficient between the two renewable generators be in $[-1, 1]$.

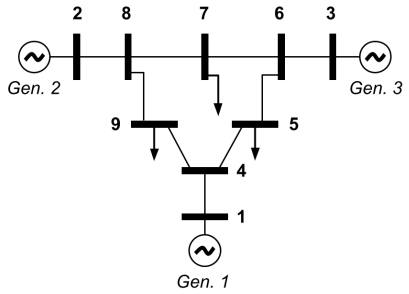

Fig. 1. Single line diagram for 9-bus system [15].

TABLE I
IEEE 9-BUS SIMULATION PARAMETERS

Parameter	Value
$P_{\text{sch},1}^{\max}$, Max schedulable power at bus 1	250 MW
c_1, Renewable construction cost	**1**
c_2, Transmission construction cost	**1**
c_3, Schedulable generation cost	**0** / MW
c_4, Load shedding cost	$0.05 \cdot$ **1** / MW

We use our planned capacity to simulate dispatch on scenarios drawn from the same distribution as those used in the planning algorithm. Fig. 2 contains our results. We found that anti-correlated renewables improved power delivery. We can see that when generator power production is correlated, the planning algorithm 1) constructs more capacity; 2) is feasible in fewer scenarios; 3) sheds more load; and 4) has increased objective value. In these tests, there were no binding transmission constraints in any scenario, so no additional transmission was built.

Next, we carry out tests where we again vary the correlation coefficient, but all lines have 50% of their prior capacity. Decreasing transmission capacity reduced the effectiveness of anti-correlated generation. Fig. 3 contains the constructed capacity, feasibility probability, load shed quantiles, LMPs, objective value, and line 1-4 constructed transmission plotted against correlation. Our algorithm only added transmission on line 1-4, which connects the schedulable generation to the network. Again, we see that increasing the correlation coefficient increases the objective value, generation constructed, and load shed quantiles. However, it also increases the feasibility probability and decreases the LMPs. While anti-correlation decreased the load shed, there were more scenarios in which small amounts of load needed to be shed to meet power balance. Additionally, the higher LMPs at lower correlations indicate greater congestion in dispatch. We conclude that we should prefer un- or anti-correlated generation, but only with sufficient transmission capacity.

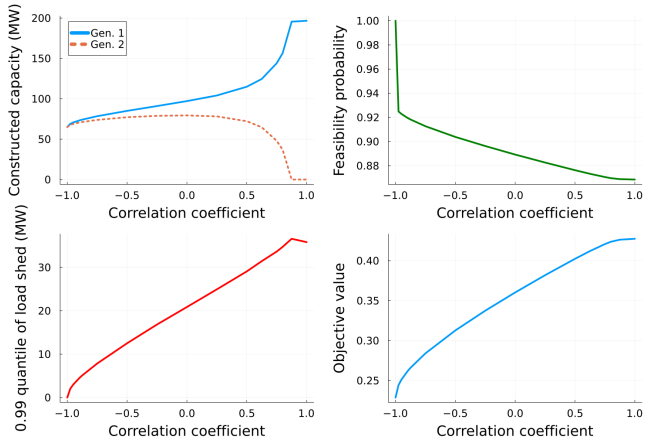

Fig. 2. Constructed renewable capacity, feasibility probability, 0.99 load shed quantile, and objective value vs. correlation coefficient with full transmission capacity.

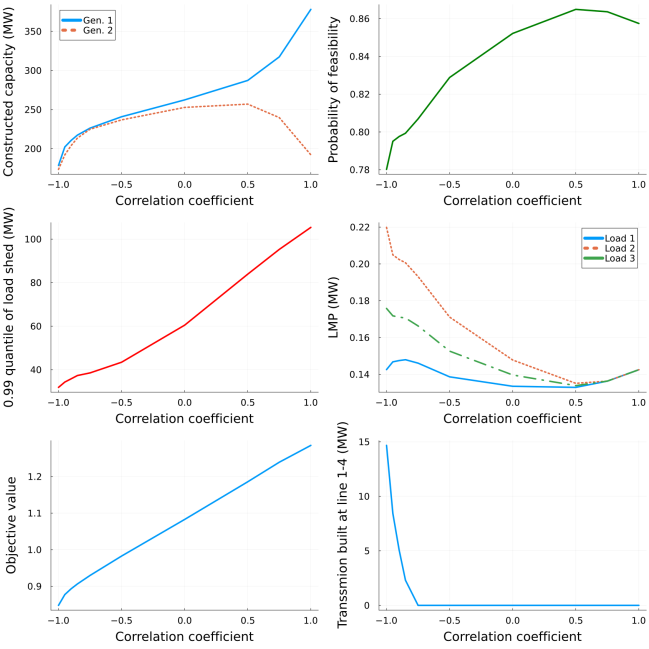

Fig. 3. Constructed renewable capacity, feasibility probability, 0.99 load shed quantile, LMPs, objective value, and transmission built on line 1-4 vs. correlation coefficient with 50% initial transmission capacity.

D. IEEE 30-Bus System

We now use a larger test case to analyze the behavior during optimal multi-period dispatch, investigating the effects of varying the schedulable generation cost c_3. We use the IEEE 30-bus system from MATPOWER [15], which has 6 generators and 18 loads, as shown in Fig. 4. Fig. 5 displays the total load in each test scenario and the mean total load. We place schedulable generators at buses 1 and 22, wind generators at buses 13, 23 and 27, and solar at bus 2. Table II contains test parameters and summary statistics for the 30-bus case. Note that solar capacity factors are low because our dataset exclusively uses data from January. We scale the cost of each renewable so that their cost per MW is equal. For our

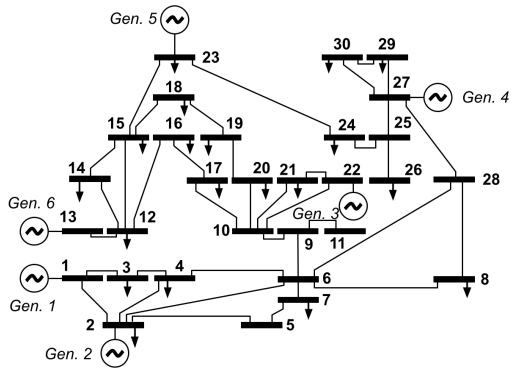

Fig. 4. Single line diagram for 30-bus system [15].

TABLE II
IEEE 30-BUS SIMULATION PARAMETERS AND SUMMARY STATISTICS

Parameter	Value
$P^{\max}_{\text{var},2}$, Max constructable capacity at bus 2	12 GW
$P^{\max}_{\text{var},13}$, Max constructable capacity at bus 13	7.4 GW
$P^{\max}_{\text{var},27}$, Max constructable capacity at bus 27	2.4 GW
$P^{\max}_{\text{var},23}$, Max constructable capacity at bus 23	2.0 GW
$P^{\max}_{\text{sch},1}$, Max schedulable power at bus 1	30 MW
$P^{\max}_{\text{sch},22}$, Max schedulable power at bus 22	30 MW
$c_1/P^{\max}_{\text{var}}$, Renewable construction cost	$2 \cdot \mathbf{1}$ / MW
c_2/f^{add}, Transmission construction cost	$4 \cdot \mathbf{1}$ / MW
c_4, Load shedding cost	$0.05 \cdot \mathbf{1}$ / MW
Summary statistic	**Value**
Capacity factor at bus 2	13.3%
Capacity factor at bus 13	47.0%
Capacity factor at bus 27	65.5%
Capacity factor at bus 23	51.2%

variability model, we obtained hourly wind, solar, and load data for January 2020 from [16], [17]. With this data, we modeled days in January by calculating hourly means and covariances for all 24 hours, giving us 24 times. We used this mean and covariance data in our planning algorithm and dispatched our system with additional planned transmission and generation on the actual data.

First, we give results for schedulable generators with no marginal cost, i.e., $c_3 = \mathbf{0}$ / MW. We find that our method generally curtails renewables and favors schedulable generators providing steady load. Table III contains the capacity added for each renewable generator and each line. Fig. 6 contains the proportion of feasible scenarios for each time period. Notably, the dips in the feasibility curve coincide with peaks in the load curve, indicating that the system is unable to satisfy peak demand. Next, we analyze the dispatch of the renewable resources. Fig. 7a contains the mean generation on each hour over all scenarios for each type of generation. We see that wind generation peaks in the morning and early afternoon, coinciding with the peaks in load. Fig. 7b contains the mean curtailment of each renewable generator in each hour over all scenarios. We see that on average, the wind generators are about 80% curtailed, and most of their energy is spilled. Meanwhile, the schedulable generators run closer

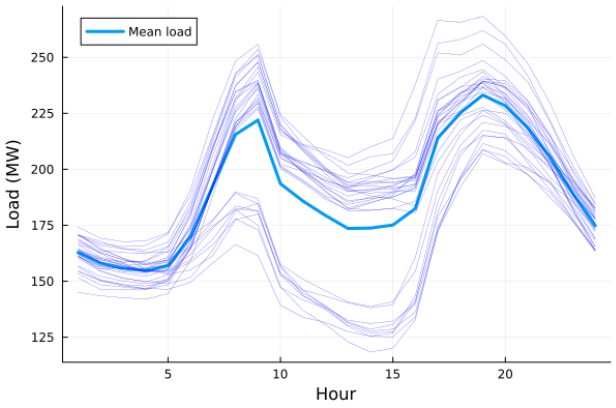

Fig. 5. Mean total load and load scenarios for 30-bus system over a day.

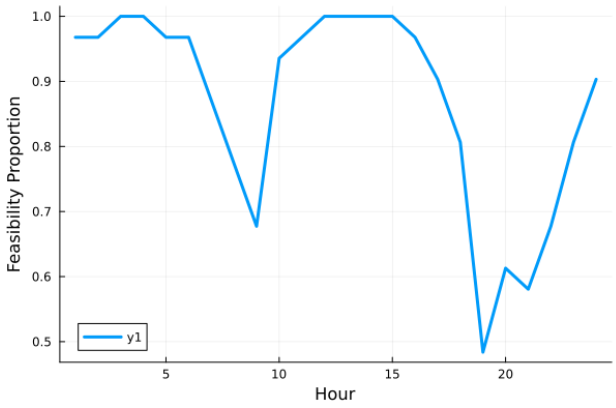

Fig. 6. Proportion of feasible periods for 30-bus system over 24 hours without schedulable generation marginal cost, i.e., $c_3 = \mathbf{0}$ / MW.

TABLE III
RESOURCES BUILT FOR 30-BUS SYSTEM WITH AND WITHOUT SCHEDULABLE GENERATION MARGINAL COST c_3

Resource	Capacity Added $c_3 = \mathbf{0}$ / MW	Capacity Added $c_3 = 0.05 \cdot \mathbf{1}$ / MW
Solar at bus 2 (Solar 1)	727.77 MW	856.65 MW
Wind at bus 27 (Wind 1)	1087.33 MW	1405.46 MW
Wind at bus 23 (Wind 2)	507.15 MW	494.27 MW
Wind at bus 13 (Wind 3)	1066.84 MW	1100.71 MW
Total generation added	*3389.09 MW*	*3857.09 MW*
Line 6-8	16.76 MW	13.66 MW
Line 12-13	20.21 MW	19.99 MW
Line 15-18	N/A	1.51 MW
Line 21-22	1.55 MW	0.22 MW
Line 15-23	16.00 MW	16.00 MW
Line 22-24	1.55 MW	11.49 MW
Line 24-25	N/A	8.41 MW
Line 25-27	3.58 MW	12.08 MW
Line 27-30	0.29 MW	0.29 MW
Line 6-28	0.41 MW	10.95 MW
Total transmission added	*60.35 MW*	*94.6 MW*

to their full capacity except during the middle of the day, during which solar produces more power.

Next, we rerun our planning and dispatch for a case where schedulable generators have a marginal cost of $c_3 = 0.01 \cdot \mathbf{1}$ / MW. We find that even though schedulable generators curtail more often, there is no appreciable change in renewable curtailment because our planning algorithm sized renewables larger. Again, Table III contains the planning results for the case with marginal cost for schedulable generation. We see that increasing the marginal cost led to the planning algorithm constructing about 470 MW more generation and 35 MW more transmission capacity. Next, we look at power generation in Fig. 8a and curtailment in Fig. 8b. Even though Fig. 8a shows that DC OPF dispatched more power from renewables, Fig. 8b shows that the curtailment of renewables did not change significantly between the two cases.

V. CONCLUSION

We have developed a stochastic optimization framework to size renewables and transmission while minimizing the cost of construction and load shedding. Our framework overbuilds renewables and curtails them during times of excess capacity. On the simpler 9-bus case, we found that anti-correlation of generation resulted in lower power variability and generation capacity needs. However, these benefits were only fully realized with sufficient transmission capacity. On the 30-bus system, we found that minimum-cost solutions relied on renewables, particularly wind, as a source of flexibility by heavily curtailing them during dispatch, even when we increased the cost of schedulable generation.

Future work includes modeling improvements, further analysis of dispatch, and comparison of renewable over-capacity with storage. Here, we modeled renewable and load variability via truncated joint normal distributions that were independent across time, and we captured spatial (not temporal) correlations. This choice may not be accurate, e.g., because we model renewable power standard deviation as scaling linearly with capacity. However, our planning algorithm could be extended to this case because our method does not assume a distribution. We could also analyze how using anti-correlation affects day-ahead dispatch, because in day-ahead dispatch, operators must account for forecast error in addition to variability. Anti-correlation may change the impact of forecast error on day-ahead dispatch and generation capacity needs. Lastly, we could extend our analysis to compare our approach to one that includes energy storage, or we could extend our planning method to co-optimize storage.

REFERENCES

[1] M. Pathak, R. Slade, P. Shukla, J. Skea, R. Pichs-Madruga, and D. Ürge-Vorsatz, "Technical Summary," in *Climate Change 2022: Mitigation of Climate Change. Contribution of Working Group III to the 6th Assessment Report of the IPCC*, P. e. a. Shukla, Ed. Cambridge, UK & New York City, USA: Cambridge University Press, 2022.

[2] *Harnessing Variable Renewables: A Guide to the Balancing Challenge*. Paris: OECD/IEA, 2011.

[3] J. Jurasz, F. Canales, A. Kies, M. Guezgouz, and A. Beluco, "A review on the complementarity of renewable energy sources: Concept, metrics, application and future research directions," *Solar Energy*, vol. 195, pp. 703–724, Jan. 2020.

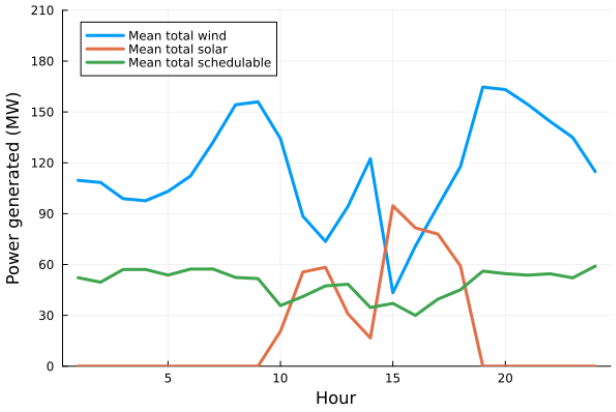

(a) Mean total generation for wind, solar, and schedulable generation.

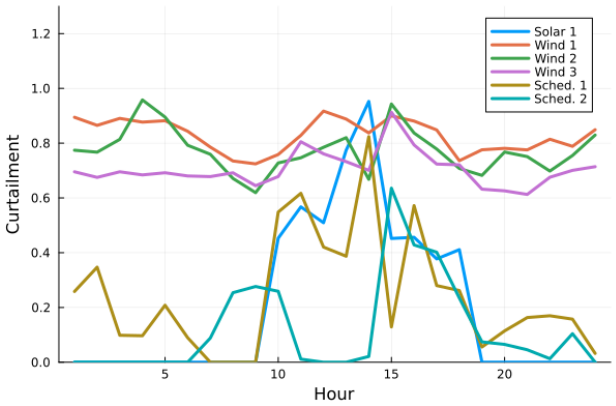

(b) Mean curtailment for each generator.

Fig. 7. Mean generation and curtailment for 30-bus test with no schedulable generation marginal cost, i.e., $c_3 = \mathbf{0}$ / MW.

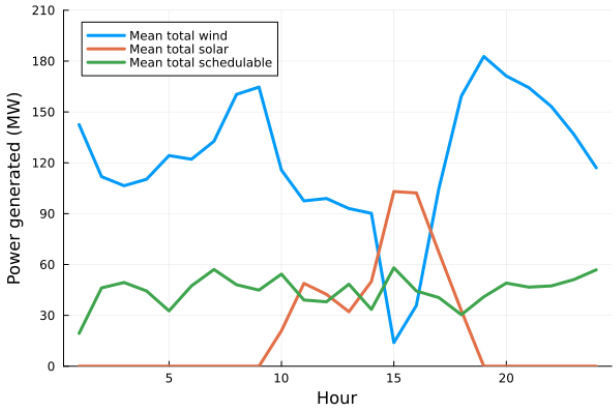

(a) Total mean generation for wind, solar, and schedulable generation.

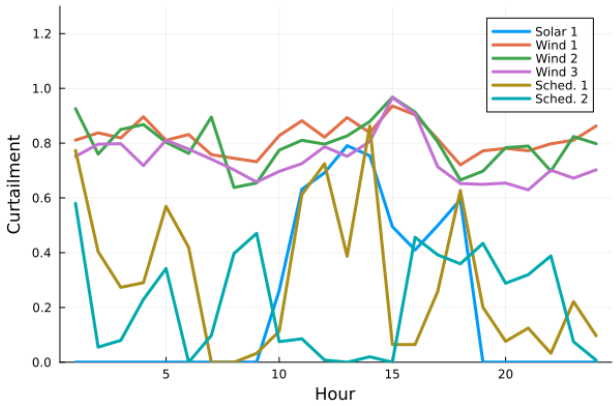

(b) Mean curtailment for each generator.

Fig. 8. Mean generation and curtailment for 30-bus test with schedulable generation marginal cost at $c_3 = 0.01 \cdot \mathbf{1}$ / MW.

[4] J. Jurasz and B. Ciapała, "Integrating photovoltaics into energy systems by using a run-off-river power plant with pondage to smooth energy exchange with the power gird," *Applied Energy*, vol. 198, pp. 21–35, Jul. 2017.

[5] D. Heide, L. von Bremen, M. Greiner, C. Hoffmann, M. Speckmann, and S. Bofinger, "Seasonal optimal mix of wind and solar power in a future, highly renewable Europe," *Renewable Energy*, vol. 35, no. 11, pp. 2483–2489, Nov. 2010.

[6] K. De Vos, J. Morbee, J. Driesen, and R. Belmans, "Impact of wind power on sizing and allocation of reserve requirements," *IET Renewable Power Generation*, vol. 7, no. 1, pp. 1–9, Jan. 2013.

[7] H. Pandžić, Y. Wang, T. Qiu, Y. Dvorkin, and D. S. Kirschen, "Near-Optimal Method for Siting and Sizing of Distributed Storage in a Transmission Network," *IEEE Transactions on Power Systems*, vol. 30, no. 5, pp. 2288–2300, Sep. 2015.

[8] Y. Zhang, S. Zhu, and A. A. Chowdhury, "Reliability Modeling and Control Schemes of Composite Energy Storage and Wind Generation System With Adequate Transmission Upgrades," *IEEE Transactions on Sustainable Energy*, vol. 2, no. 4, pp. 520–526, Oct. 2011.

[9] D. Bienstock, M. Chertkov, and S. Harnett, "Chance-Constrained Optimal Power Flow: Risk-Aware Network Control under Uncertainty," *SIAM Review*, vol. 56, no. 3, pp. 461–495, Jan. 2014.

[10] M. Vrakopoulou, K. Margellos, J. Lygeros, and G. Andersson, "A Probabilistic Framework for Reserve Scheduling and N-1 Security Assessment of Systems With High Wind Power Penetration," *IEEE Transactions on Power Systems*, vol. 28, no. 4, pp. 3885–3896, Nov. 2013.

[11] L. Boffino, A. J. Conejo, R. Sioshansi, and G. Oggioni, "A two-stage stochastic optimization planning framework to decarbonize deeply electric power systems," *Energy Economics*, vol. 84, p. 104457, Oct. 2019.

[12] Y. Liu, R. Sioshansi, and A. J. Conejo, "Multistage Stochastic Investment Planning With Multiscale Representation of Uncertainties and Decisions," *IEEE Transactions on Power Systems*, vol. 33, no. 1, pp. 781–791, Jan. 2018.

[13] C. Coffrin, R. Bent, K. Sundar, Y. Ng, and M. Lubin, "Powermodels.jl: An open-source framework for exploring power flow formulations," in *2018 Power Systems Computation Conference*, June 2018, pp. 1–8.

[14] I. Dunning, J. Huchette, and M. Lubin, "Jump: A modeling language for mathematical optimization," *SIAM Review*, vol. 59, no. 2, pp. 295–320, 2017.

[15] R. D. Zimmerman, C. E. Murillo-Sanchez, and R. J. Thomas, "MATPOWER: Steady-State Operations, Planning, and Analysis Tools for Power Systems Research and Education," *IEEE Transactions on Power Systems*, vol. 26, no. 1, pp. 12–19, Feb. 2011.

[16] K. Rojowsky and A. Gothandaraman, "Hourly Wind and Solar Generation Profiles," Electric Reliability Council of Texas, Tech. Rep. 21-03-036658, Sep. 2021. [Online]. Available: https://www.ercot.com/files/docs/2021/12/07/Report_ERCOT_1980-2020_WindSolarDGPVGenProfiles.pdf

[17] "Backcasted (Actual) Load Profiles - Historical." [Online]. Available: https://www.ercot.com/mktinfo/loadprofile/alp